Influences of Out-Of-Plane Lattice Alignment on the OFET Performance of TIPS-PEN Crystal Arrays

Kuan-Yi Wu,[†] Chou-Ting Hsieh,[†] Liang-Hsun Wang,[†] Chih-Hao Hsu,[‡] Shu-Ting Chang,[†] Shih-Ting Lan,[†] Yi-Fan Huang,[†] Yu-Ming Chen,[‡] and Chien-Lung Wang*,[†]

[†]Department of Applied Chemistry, National Chiao Tung University, 1001 Ta Hsueh Rd., Hsinchu, Taiwan 30010

[‡]Department of Polymer Science, College of Polymer Science and Polymer Engineering, The University of Akron, Akron, Ohio 44325, United States

Ⓢ Supporting Information

ABSTRACT: In organic field-effect transistors (OFETs), the quality of charge-transport pathway, controlled by crystal structures of organic semiconductors (OSCs), strongly affects the performance of the device. To achieve higher charge mobility, solution-processed single-crystal (SPSC) techniques have been used to decrease crystal defects by aligning the crystals of OSCs in the in-plane direction. Nonetheless, through SPSC techniques, whether the crystalline lattices are well-aligned in the out-of-plane direction and how the out-of-plane lattice misorientaion affects OFET performances remain unclear. Here, a characterization protocol based on polarized optical microscope, X-ray diffraction, and electron diffraction is established to identify the lattice structure, the in-plane and out-of-plane lattice alignment in the crystal array of 6,13-bis(triisopropylsilylethynyl)pentacene (TIPS-PEN). Regardless of the solvents used in the PDMS-assisted crystallization, the characterization protocol confirms that all the crystal arrays share the same lattice structure (form I phase), and have similar in-plane lattice alignment. However, TIPS-PEN molecules have sufficient time to unify their out-of-plane orientation and prevent the formation of low angle grain boundary (LAGB) during crystal growth if high boiling temperature solvents are used. The improved out-of-plane lattice alignment increases the hole mobility and decreases the performance fluctuations of devices. The results confirm that the out-of-plane lattice alignment significantly impacts the performance of the devices and the reproducibility of the solution-processed TIPS-PEN OFETs.
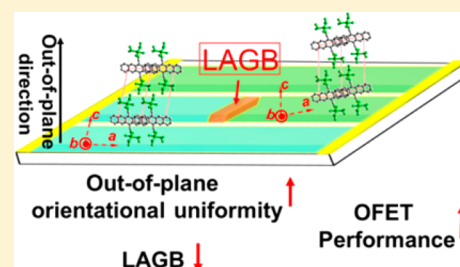
Morphological parameters at different length scales are determinative factors affecting the performance of organic semiconductor (OSC) thin films.[1−3] Within a crystal lattice, charge mobility (μ) of an OSC is influenced by molecular packing, which determines the degrees of intermolecular π-overlapping and transfer integral among the molecules.[4,5] Modification of the molecular structures of OSCs and/or adjustment of the processing conditions optimizes the positions of the frontier orbitals and packing structures of an OSC, and consequently the device performance.[6−10] Above the length scale of a crystal lattice, μ is affected by thin-film morphology.[11−13] For instance, grain boundaries, the interface separating the randomly oriented single-crystal domains, are the trapping sites of charges, which hinder the charge transport in crystalline films.[14−17] In order to decrease the density of the grain boundary, solution-processed single-crystal (SPSC) techniques have been developed for the preparation of oriented single-crystal arrays.[18−22] The increased crystal size and the unified in-plane crystal orientation promote the hole mobility (μ_h) of 6,13-bis(triisopropylsilylethynyl)-pentacene (TIPS-PEN) and electron mobility of (μ_e) of C_{60} to over 10 cm²/(V s).[23,24] Significant increases of μ are also found in the thin films of many conjugated polymers and oligomers, when the in-plane orientation is improved.[25]

Crystals formed by organic molecules (i.e., molecular crystals) are different from those composed of ionic compounds. The intermolecular interactions in molecular crystals are weaker and short-range as compared to the stronger and long-range Coulombic interactions in ionic crystals. Due to the weak intermolecular interactions, molecules reaching the growth front of a molecular crystal experience only weak orientating forces.[26] Thus, in the crystal structure, locations where motifs are missing or irregularly placed are more likely to form structural defects during the growth of molecular crystals. Structural defects in a crystal can be categorized into point defects, line defects or dislocations, and planar defects or stacking faults. A stacking fault would further result in twinned crystals in which the two neighboring crystalline domains meet along a composition plane; a series of edge dislocation along a boundary plane creates a low-angle grain boundary (LAGB), where two neighboring crystalline domains grow at an angle (θ) to each other. Because molecules at the structural defects are off their equilibrium lattice sites, they influence the migration of charges in a molecular crystal. Despite the fact that structural defects are energetically
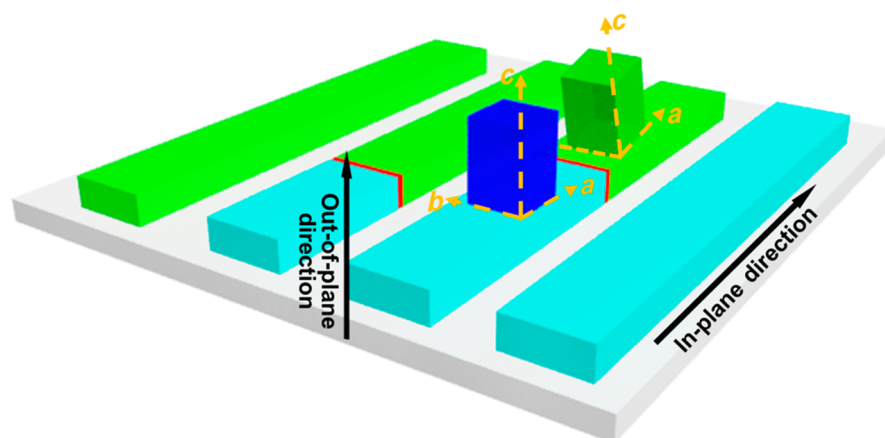
Figure 1. Illustration of out-of-plane misorientation in the crystal arrays of OSCs with a great in-plane orientation. The blue and green crystal domains have the same lattice structure but with different out-of-plane lattice orientation (blue and green blocks). The LAGB (red line) separates the crystalline domains (blue and green blocks), which are misoriented in the out-of-plane direction.
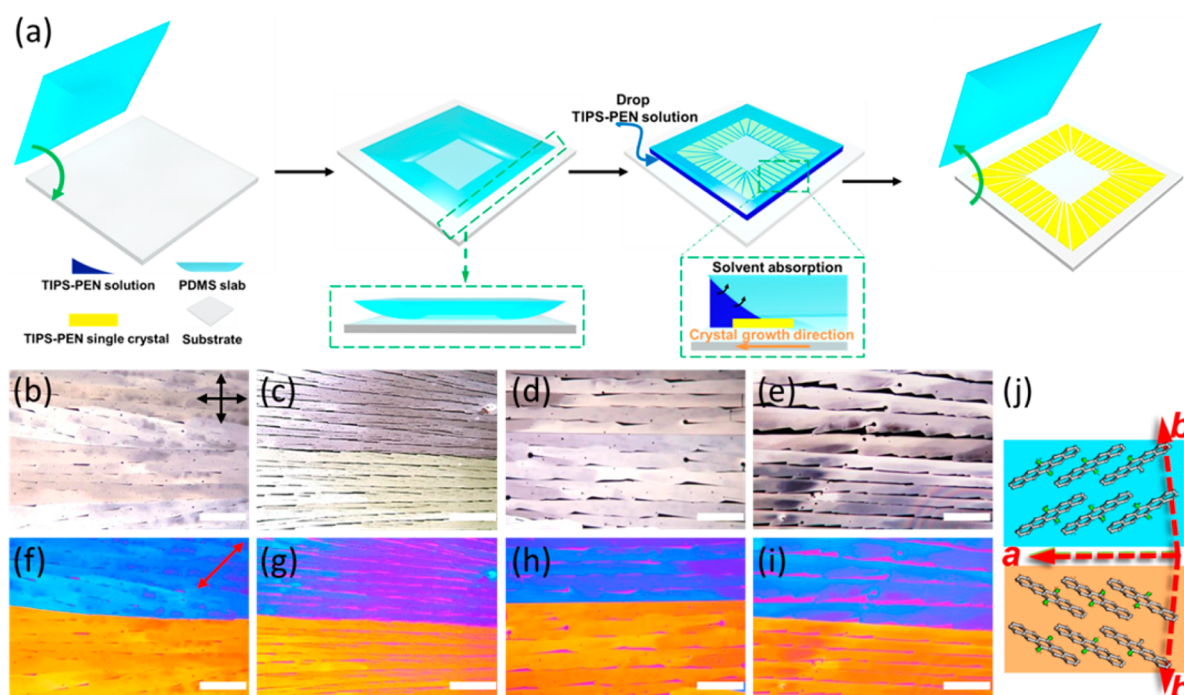

Figure 2. (a) Schematic illustration of PDMS-assisted crystallization method (PAC). (b−j) POM images of TIPS-PEN crystal arrays grown by the PAC method from (b,f) DCM, (c,g) CS$_2$, (d,h) Tol, and (e,i) CB. POM images are captured (b−e) without and (f−i) with the retardation plate. (j) Illustration of the molecular orientation of TIPS-PEN lattice in blue and yellow domains (without side chains). The black arrows in (b) indicate the polarization direction of the polarizer (P) and analyzer (A), and the red arrow in (f) shows the slow axis of the full-wavelength retardation plate. The scale bar is 50 μm.

unfavorable, they can be trapped kinetically in a crystal during the process of crystal growth.[26,27]

Although SPSC methods are powerful in regulation of the in-plane lattice orientation, whether or not the lattice misorientation could occur in the out-of-plane direction remains unclear. Like the in-plane misorientation of crystalline domains, the misorientation in the out-of-plane direction (Figure 1) could also create grain boundaries between the neighboring crystalline domains, which breaks the charge-transporting pathway and affects the μ of OSC thin films. Until now, the out-of-plane misorientation in the crystal arrays of OSCs has yet to be carefully examined. Thus, in this study, we first identified the out-of-plane misoriented crystalline domains

by electron diffraction (ED) techniques, and deduced the orientational parameter of TIPS-PEN crystal arrays in the out-of-plane direction via analyzing the grazing incidence X-ray diffraction (GIXD) patterns. The diffraction results clearly revealed the misoriented crystalline domains within the individual crystal of the TIPS-PEN crystal arrays, and showed the existence of the out-of-plane low-angle grain boundary (LAGB in Figure 1) along the long axis of the in-plane oriented crystals. In addition, the degree of out-of-plane lattice misorientation can be controlled by processing conditions. Using the poly(dimethylsiloxane) (PDMS)-assisted crystallization (PAC) method,[28] we examined the growth of the crystal arrays under a spectrum of solvents with boiling temperatures
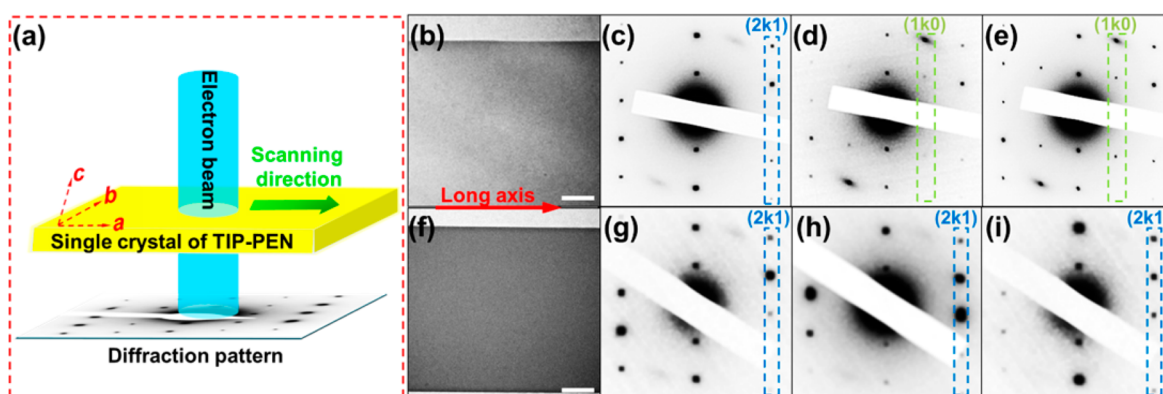
Figure 3. (a) Schematic illustration of the ED scanning experiment. TEM images of an individual crystal in the TIP-PEN crystal arrays prepared from (b) DCM and (f) Tol. The ED patterns were taken along the long axis of the crystal prepared from (c−e) DCM and (g−i) Tol. In the crystal prepared from DCM, the (2k1) diffractions are observed in (c), whereas the (1k0) diffractions are seen in (d) and (e). Thus, the pattern in (c) is denoted as ED-A, and those in (d) and (e) are denoted as ED-B. In the crystal prepared from Tol, only ED-A is observed. The scale bar in (b) and (f) is 1 μm.

(T_b) ranging from 40 °C (dichloromethane) to 131 °C (chlorobenzene). With the assistance of the PAC method, it was found that the degree of out-of-plane misorientation can be effectively reduced in the crystal arrays prepared from the high T_b solvents. As a result, the improved μ_hs and the decreased fluctuations of performance show the significant role of the out-of-plane crystal orientation and LAGB in the performances and the reproducibility of the OFET devices.

Prior to investigating the out-of-plane crystal orientation in a crystal array, the crystal arrays of TIPS-PEN were fabricated through the PAC method as shown in Figure 2a. Since PDMS is compatible with many solvents,[29] we used it as a solvent sponge in the PAC method to induce supersaturation, nucleation, and crystal growth from the TIPS-PEN solutions. The elongated crystal arrays of TIPS-PEN shown in Figure 2 were successfully prepared from dichloromethane (DCM) (T_b: 40 °C), carbon disulfide (CS$_2$) (T_b: 46 °C), toluene (Tol) (T_b: 110 °C), and chlorobenzene (CB) (T_b: 131 °C) at room temperature without sophisticated shearing systems and patterned surfaces.

Molecular packing of TIPS-PEN is sensitive to the processing conditions such as temperature, shearing rate, solvent property, and thickness confinement. Five different lattice structures have been reported for TIPS-PEN crystals prepared from different procedures.[30,31] Thus, before identifying the influences of lattice orientation, we combined the ED patterns (Figure S2a−d) with the GIXD patterns (Figure S2e−l) to construct the three-dimensional reciprocal lattice of the TIPS-PEN crystals, so that the crystal structures of TIPS-PEN produced from different solvents can be identified. As illustrated in Figure S1, the top projection of the reciprocal lattice can be shown by the ED pattern. The lateral and end projections of the reciprocal lattice can be obtained from the perpendicular and parallel GIXD patterns, respectively. In Figure S2, the lattice parameters [$a = 7.74$ Å, $b = 7.67$ Å, $\gamma = 82.0°$] can be deduced from the ED patterns; [$a = 7.74$ Å, $c = 17.03$ Å, $\beta = 77.0°$] and [$b = 7.67$ Å, $c = 17.03$ Å, $\alpha = 88.7°$] can be deduced from the perpendicular and the parallel GIXD patterns, respectively. These lattice parameters of the crystal arrays prepared from different solvents are summarized in Table S1. In the PAC method, TIPS-PEN molecules form the identical lattice structure from different solvents, and compared to the five reported crystal lattices of TIPS-PEN, it is confirmed that the

PAC method produces the triclinic Form I crystal of TIPS-PEN.[30]

Knowing that solvent properties have no influence on the lattice structure of the TIPS-PEN crystal arrays, we further examined the in-plane and out-of-plane orientation of the crystal arrays. Under a polarized optical microscope (POM), all the crystal arrays show great in-plane orientation regardless of the use of solvents (Figure 2). In addition, with a full-wavelength retardation plate, the approximate molecular orientations of TIPS-PEN in the crystal arrays can be revealed under a POM. As illustrated in Figure 2j, TIPS-PEN molecules aligned roughly along the upper-right and lower-left direction showed a blue color, whereas those along the upper-left and lower-right direction showed a yellow color. ED patterns then gave a more precise molecular orientation by specifying the relationship between the lattice axes of TIPS-PEN and the growth axis of the crystal. In Figure 3, the (100) diffraction spot is observed on the growth axis, and the (010) spot is positioned at a direction nearly perpendicular to the growth axis. Thus, after superimposing the *ab* lattice of TIPS-PEN onto the crystal, the exact in-plane molecular orientation of TIPS-PEN molecules can be identified. Combining the POM and ED results, we found that the angle between the molecular long-axes of TIPS-PENs and the crystal-growth axis is 30°. Furthermore, the neighboring blue-colored and yellow-colored crystals in Figure 2f−i are a pair of twin crystals, sharing their (010) planes as the twin boundary in the in-plane direction.[26,32] To identify the origin of the twin boundary, we recorded a video (Video S1) and found that the twin boundary formed at the nucleation stage of the PAC process. Although the following crystal-growth process can align the *a*-axes of the neighboring crystals along the growth direction, it cannot regulate the directions of the *b*-axes, which have already been determined during the nucleation stage. Therefore, unless the nucleation region is treated with triangular-shaped hydrophilic/hydrophobic surface pattern in advance, the formation of the twin boundaries in the crystal array of TIPS-PEN will be inevitable.[23]

To investigate the out-of-plane orientation of crystal arrays, we used the electron beam in transmission electron microscopy (TEM) to scan an individual crystal along its long axis as illustrated in Figure 3a. Surprisingly, at least two types of ED patterns (ED-A and ED-B) were found in the crystals prepared
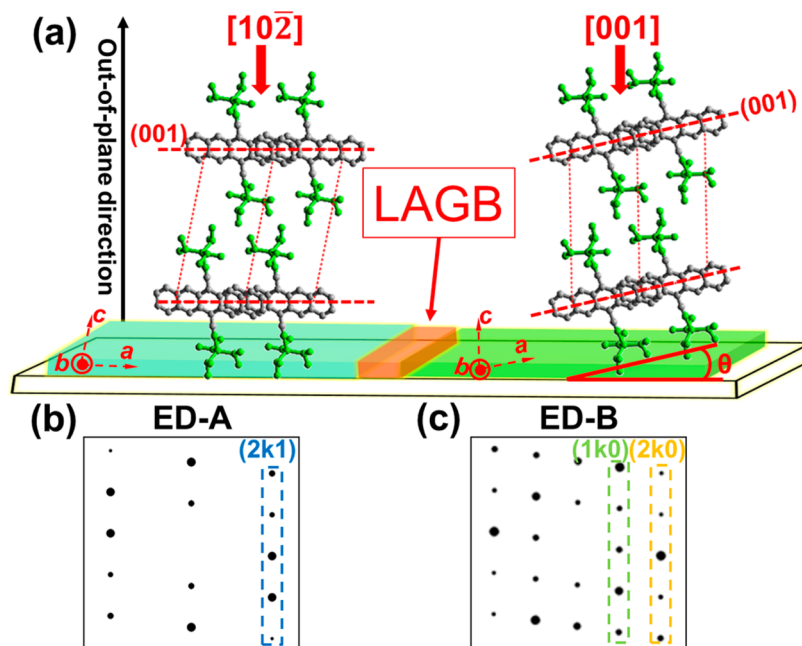
Figure 4. (a) Schematic illustration of out-of-plane lattice misorientation and LAGB along the long axis of a TIPS-PEN crystal. The domains A and B are indicated with the blue and green color, respectively. The simulated (b) $[10\bar{2}]$ zone and (c) $[001]$ zone ED patterns (ED-A and ED-B) are generated from the Form I TIPS-PEN crystal structure. The misorientation angle between the domain A and B is less than 13° which is confirmed by the simulated ED patterns and the tilting experiment in Figure S4.
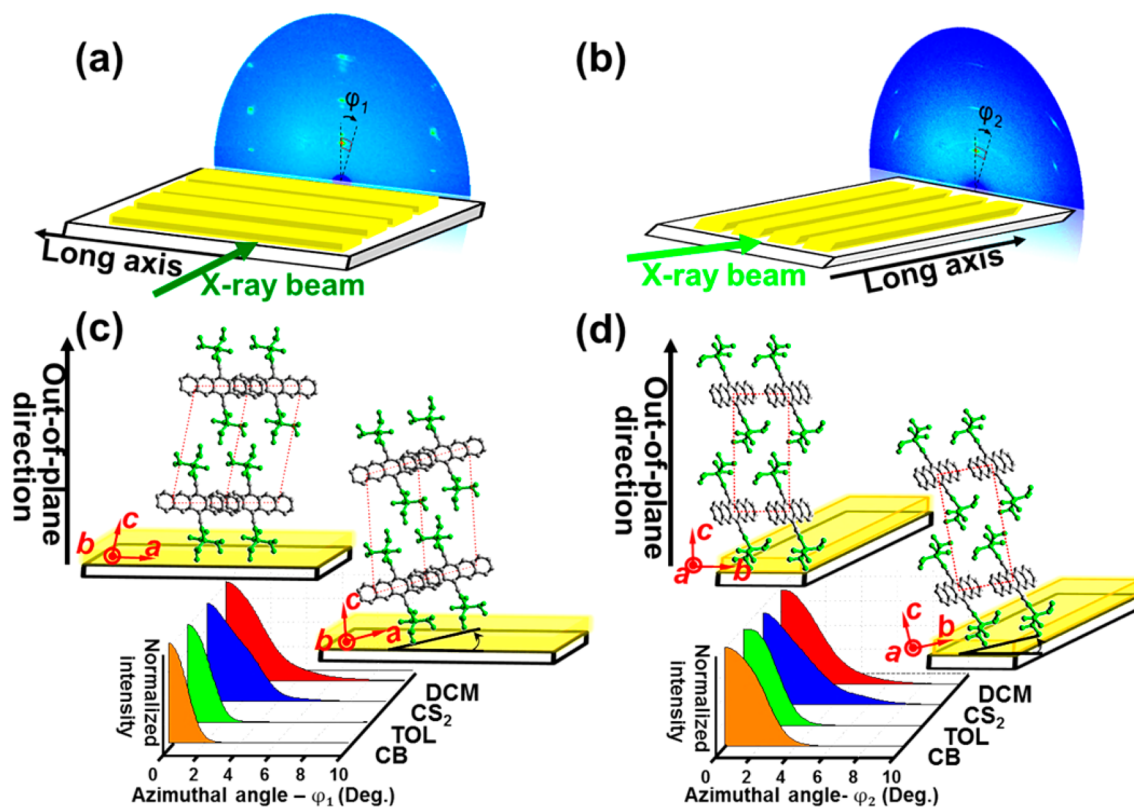

Figure 5. Schematic illustrations of (a) the perpendicular and (b) the parallel GIXD setup. The perpendicular setup provides morphological information along the long axis of TIPS-PEN crystal arrays, while the parallel setup gives morphological information along the short axis. (c) and (d) show the illustrations of out-of-plane orientation of TIPS-PEN on a Si substrate, derived from the plots of the intensity of the (001) diffraction which is the function of the azimuthal angles, φ_1 and φ_2 along the long axis and the short axis of the crystal array, respectively.

from low T_b solvents, including DCM (Figure 3b–e) and CS$_2$ (Figure S3a–d). The difference between the two diffraction patterns is that in ED-A (Figure 3c), the (2k1) diffractions were observed, whereas (1k0) diffractions were found in ED-B (Figure 3d,e). From the simulated diffraction patterns of the Form I TIPS-PEN crystal (Figure 4b,c), it is confirmed that the

ED-A pattern is generated when the electron beam is nearly along the $[10\bar{2}]$ zone of the TIPS-PEN lattice, while the ED-B pattern is generated when the electron beam is away from $[10\bar{2}]$ zone and approaching to the $[001]$ zone. The distinct ED patterns found in an individual crystal indicate the presence of the lattice misorientation in the out-of-plane direction. In order to estimate the misorientation angle between the crystalline domains that give ED-A and ED-B, a tilting experiment in TEM was carried out (Figure S4). We took the short axis of a TIPS-PEN crystal as the rotation axis, and found that the crystalline domain, which generates ED-A, can produce ED-B after tilting the crystal for 13° along its short axis. The tilting experiment thus validates the misorientation angle between domain A and B within an individual crystal is less than 13°, which is consistent with (001) intensity distribution of GIXD patterns (Figure 5c). In order to elaborate on how the lattices misaligned in the out-of-plane direction, we placed two enlarged TIPS-PEN lattices along the long axis of a TIPS-PEN crystal as shown in Figure 4a. With the out-of-plane direction taken as a reference axis, it is clear that the normal vector of the (001) plane of the TIPS-PEN lattice is parallel to the out-of-plane direction in domain A, but tilted by an angle (θ) less than 13° from the out-of-plane direction in domain B. Thus, the ED characterization shows that the crystalline domains within an individual crystal align differently in the out-of-plane direction, indicating that a grain boundary is present between the two neighboring crystalline domains. Since the misorientation angle between domain A and B is less than 15°, the grain boundary is defined as the out-of-plane LAGB.[33,34] Obviously, the presence of the LAGBs within the individual TIPS-PEN crystal slices the TIPS-PEN crystal into several "crystalline blocks", which could be potentially detrimental to the charge transport.

In contrast, only the ED-A pattern was observed during the ED scanning along the long axis of the crystals prepared from Tol and CB (Figure 3f–i and Figure S3e–h). The result indicates the crystalline domains are well-aligned in the out-of-plane direction. High T_b solvents, such as Tol and CB, provide longer growth time for the crystallization of the crystal arrays (Table S2), allowing the TIPS-PEN molecules to adjust their molecular orientations in the way that the triisopropylsilyle-thynyl groups of TIPS-PEN molecules are in close contact with the substrate (Domain A of Figure 4). On the contrary, lower T_b solvents, such as DCM and CS_2, do not provide sufficient time for TIPS-PEN molecules to optimize their orientation, which causes the formation of tilted lattices and nonuniform out-of-plane orientation in the crystal arrays.

Although the ED technique can be used to identify the presence of the LAGB in the crystal arrays, it cannot represent the overall out-of-plane alignment of the crystalline domains, since the sampling area in the ED experiments is relatively small. To estimate how well the crystalline domains are aligned along the out-of-plane direction, we first collected the perpendicular (Figure 5a) and parallel (Figure 5b) GIXD patterns of the TIPS-PEN crystal arrays. The intensity of the (001) diffraction (at $q_z = 3.8$ nm^{-1}) is then plotted against the azimuthal angles φ_1 and φ_2. The obtained intensity profiles in Figure 5c and d are used as an index for the distribution of out-of-plane crystal orientation. In Figure 5c and d, the crystal arrays prepared from DCM and CS_2 gave the dispersed intensity of the (001) diffraction with wider φ_1 and φ_2 angles. Because the (001) diffraction is located at the normal direction of the (001) plane, the broader intensity distribution in the

DCM and CS_2 cases represents a poorer crystal alignment in the out-of-plane direction. Furthermore, the broader diffraction profiles in both the φ_1 and φ_2 directions also suggest that the misorientation of crystalline domains can be found along both the long and short axes of the TIPS-PEN crystals as illustrated in Figure 5c and d, respectively. To further quantify the extent of out-of-plane orientation, we calculated the Herman's orientation parameters from the azimuthal intensity profiles of the (001) diffraction. The orientation parameter (f) is defined as eqs 1 and 2

$$f = (3\langle \cos^2 \varphi \rangle - 1)/2 \tag{1}$$

$$\langle \cos^2 \varphi \rangle = \frac{\int_0^{\pi/2} I(\varphi) \cos^2 \varphi \, \sin \varphi \, d\varphi}{\int_0^{\pi/2} I(\varphi) \sin \varphi \, d\varphi} \tag{2}$$

where φ is the azimuthal angle and $I(\varphi)$ is the intensity of (001) diffraction as the function of azimuthal angle.[35] At $f_{001} = 1$, all the crystalline domains in the crystal array have their normal vector of (001) plane oriented along the out-of-plane direction, whereas at $f_{001} = 0$, the orientation of the (001) normal is completely random. Table S3 shows the f_{001} values deduced both from the φ_1 and φ_2 azimuthal profiles of the (001) diffraction. In both the φ_1 and φ_2 intensity profiles, crystal arrays prepared from Tol and CB have higher f_{001} values, indicating that high T_b solvents facilitate the formation of the better oriented TIPS-PEN crystal arrays. Notably, in the Tol and CB cases, the crystal arrays have nearly perfect out-of-plane crystal orientation along the growth direction of the crystal arrays as demonstrated by the f_{001} value of 0.99 in the φ_1 profile. In addition, the f_{001} values obtained from the φ_2 profiles (Table S3) are lower than those obtained from the φ_1 profile, indicating that in the PAC process, unifying the out-of-plane orientation of the bc lattices is more difficult than unifying the orientation of the ac lattices. The azimuthal intensity analysis of the GIXD pattern thus allows the quantitative evaluation of the out-of-plane alignment of crystalline domains in the crystal array. The GIXD analysis also show that when Tol and CB (the high T_b solvents) are used in the PAC process, TIPS-PEN molecules are better aligned in the out-of-plane direction, which is consistent with the conclusion from the ED analysis.

The μ_h values of the crystal arrays were evaluated in the OFETs with the top-contact and bottom-gate geometry. The growth directions of the crystal arrays were placed along the source/drain direction of OFET devices. The OFET character-istics of the crystal arrays were shown in Figure S5 and summarized in Table 1. As shown in Table 1, OFET devices fabricated from the high T_b solvents gave higher μ_h values and

Table 1. OFET Device Characteristics of the TIPS-PEN Crystal Arrays Prepared from Different Solvents

solvent[a]	μ_{avg}[b] (μ_{max}) (cm^2 V^{-1} s^{-1})	coefficient of variation (CV)	$I_{on/off}$	V_T (V)
dichloromethane	0.50 (0.97)	54%	10^4–10^6	0 to −35
carbon disulfide	0.49 (0.93)	61%	10^3–10^5	5 to −25
toluene	1.47 (2.00)	27%	10^5–10^6	0 to −30
chlorobenzene	1.01 (1.96)	29%	10^4–10^6	0 to −30

[a]Concentration = 2 mg mL^{-1}. [b]Average value of over 20 devices.

lower coefficients of variation (CV; 100% × standard deviation/mean).[36] The crystal arrays prepared from Tol and CB delivered highest μ_h values of 2.00 and 1.96 cm^2 V^{-1} s^{-1}, respectively, which are comparable with the highest μ_h reported from the Form I TIPS-PEN crystals.[37] Note that all the crystal arrays prepared from different solvents share the same lattice structure, and have similar uniformity of in-plane orientation as indicated by the crystallographic data in Table S1 and the POM images (Figure 2). Thus, the out-of-plane crystal orientation is the key parameter to cause the variations in the μ_h of the crystal arrays. The high T_b solvents allow the TIPS-PEN molecules to reach a high out-of-plane orientational uniformity (i.e., high f_{001}), and reduce the density of the LAGBs (Figure 4 and Figure 5). As a result, the higher μ_h values and higher performance reproducibility of the OFET devices were delivered by the crystal arrays prepared from the high T_b solvents (Tol and CB).

In summary, LAGB in the TIPS-PEN crystal arrays, which separates the crystalline domains with different out-of-plane orientation, were identified by a scanning ED technique. The degree of out-of-plane misorientation in the crystal arrays was quantified by the orientation parameter of the (001) diffraction (f_{001}) in GIXD patterns. High T_b solvents, such as Tol and CB, were found to provide more time in the PAC process for the TIPS-PEN molecules to unify their out-of-plane orientation, and led to the formation of highly oriented crystal arrays with f_{001} = 0.99. The improved out-of-plane orientational uniformity enhanced the μ_h, and decreased the performance fluctuations of the TIPS-PEN OFETs. This study thus revealed the important role of the out-of-plane orientational uniformity in the performances and the reproducibility of the solution-processed OFETs.

ASSOCIATED CONTENT

Ⓢ Supporting Information

The Supporting Information is available free of charge on the ACS Publications website at DOI: 10.1021/acs.cgd.6b01391.

> Experimental Details, crystal structure characterization, ED scanning experiment, tilting experiment, orientation parameter calculations and transistor device characterizations (PDF)
> Video showing twin boundary formation at the nucleation stage (AVI)

AUTHOR INFORMATION

Corresponding Author

*E-mail: kclwang@nctu.edu.tw.

Notes

The authors declare no competing financial interest.

REFERENCES

(1) Dong, H.; Fu, X.; Liu, J.; Wang, Z.; Hu, W. Adv. Mater. 2013, 25, 6158.
(2) Hiszpanski, A. M.; Loo, Y.-L. Energy Environ. Sci. 2014, 7, 592.
(3) Mas-Torrent, M.; Rovira, C. Chem. Rev. 2011, 111, 4833.
(4) Chung, H.; Diao, Y. J. Mater. Chem. C 2016, 4, 3915.
(5) Huang, C.-F.; Wu, S.-L.; Huang, Y.-F.; Chen, Y.-C.; Chang, S.-T.; Wu, T.-Y.; Wu, K.-Y.; Chuang, W.-T.; Wang, C.-L. Chem. Mater. 2016, 28, 5175.
(6) Mei, J.; Diao, Y.; Appleton, A. L.; Fang, L.; Bao, Z. J. Am. Chem. Soc. 2013, 135, 6724.
(7) Wang, C.; Dong, H.; Hu, W.; Liu, Y.; Zhu, D. Chem. Rev. 2012, 112, 2208.
(8) Chen, J.; Shao, M.; Xiao, K.; Rondinone, A. J.; Loo, Y. L.; Kent, P. R.; Sumpter, B. G.; Li, D.; Keum, J. K.; Diemer, P. J.; Anthony, J. E.; Jurchescu, O. D.; Huang, J. Nanoscale 2014, 6, 449.
(9) Hiszpanski, A. M.; Baur, R. M.; Kim, B.; Tremblay, N. J.; Nuckolls, C.; Woll, A. R.; Loo, Y. L. J. Am. Chem. Soc. 2014, 136, 15749.
(10) Stevens, L. A.; Goetz, K. P.; Fonari, A.; Shu, Y.; Williamson, R. M.; Brédas, J.-L.; Coropceanu, V.; Jurchescu, O. D.; Collis, G. E. Chem. Mater. 2015, 27, 112.
(11) Lee, S. S.; Loo, Y. L. Annu. Rev. Chem. Biomol. Eng. 2010, 1, 59.
(12) Rivnay, J.; Jimison, L. H.; Northrup, J. E.; Toney, M. F.; Noriega, R.; Lu, S.; Marks, T. J.; Facchetti, A.; Salleo, A. Nat. Mater. 2009, 8, 952.
(13) Rivnay, J.; Mannsfeld, S. C.; Miller, C. E.; Salleo, A.; Toney, M. F. Chem. Rev. 2012, 112, 5488.
(14) Chwang, A. B.; Frisbie, C. D. J. Appl. Phys. 2001, 90, 1342.
(15) Laquindanum, J. G.; Katz, H. E.; Lovinger, A. J.; Dodabalapur, A. Chem. Mater. 1996, 8, 2542.
(16) Ly, T. H.; Perello, D. J.; Zhao, J.; Deng, Q.; Kim, H.; Han, G. H.; Chae, S. H.; Jeong, H. Y.; Lee, Y. H. Nat. Commun. 2016, 7, 10426.
(17) Mladenović, M.; Vukmirović, N.; Stanković, I. J. Phys. Chem. C 2013, 117, 15741.
(18) Becerril, H. A.; Roberts, M. E.; Liu, Z.; Locklin, J.; Bao, Z. Adv. Mater. 2008, 20, 2588.
(19) Fan, C.; Zoombelt, A. P.; Jiang, H.; Fu, W.; Wu, J.; Yuan, W.; Wang, Y.; Li, H.; Chen, H.; Bao, Z. Adv. Mater. 2013, 25, 5762.
(20) Jang, J.; Nam, S.; Im, K.; Hur, J.; Cha, S. N.; Kim, J.; Son, H. B.; Suh, H.; Loth, M. A.; Anthony, J. E.; Park, J.-J.; Park, C. E.; Kim, J. M.; Kim, K. Adv. Funct. Mater. 2012, 22, 1005.
(21) Pisula, W.; Menon, A.; Stepputat, M.; Lieberwirth, I.; Kolb, U.; Tracz, A.; Sirringhaus, H.; Pakula, T.; Müllen, K. Adv. Mater. 2005, 17, 684.
(22) Diao, Y.; Shaw, L.; Bao, Z.; Mannsfeld, S. C. B. Energy Environ. Sci. 2014, 7, 2145.
(23) Diao, Y.; Tee, B. C.; Giri, G.; Xu, J.; Kim, D. H.; Becerril, H. A.; Stoltenberg, R. M.; Lee, T. H.; Xue, G.; Mannsfeld, S. C.; Bao, Z. Nat. Mater. 2013, 12, 665.
(24) Li, H.; Tee, B. C.; Cha, J. J.; Cui, Y.; Chung, J. W.; Lee, S. Y.; Bao, Z. J. Am. Chem. Soc. 2012, 134, 2760.
(25) Luo, C.; Kyaw, A. K.; Perez, L. A.; Patel, S.; Wang, M.; Grimm, B.; Bazan, G. C.; Kramer, E. J.; Heeger, A. J. Nano Lett. 2014, 14, 2764.
(26) Wright, J. D. Molecular crystals; Cambridge University Press, 1995.
(27) Jiang, H.; Kloc, C. MRS Bull. 2013, 38, 28.
(28) Wu, K. Y.; Wu, T. Y.; Chang, S. T.; Hsu, C. S.; Wang, C. L. Adv. Mater. 2015, 27, 4371.
(29) Lee, J. N.; Park, C.; Whitesides, G. M. Anal. Chem. 2003, 75, 6544.
(30) Diao, Y.; Lenn, K. M.; Lee, W.-Y.; Blood-Forsythe, M. A.; Xu, J.; Mao, Y.; Kim, Y.; Reinspach, J. A.; Park, S.; Aspuru-Guzik, A. n.; et al. J. Am. Chem. Soc. 2014, 136, 17046.
(31) Giri, G.; Li, R.; Smilgies, D. M.; Li, E. Q.; Diao, Y.; Lenn, K. M.; Chiu, M.; Lin, D. W.; Allen, R.; Reinspach, J.; Mannsfeld, S. C.; Thoroddsen, S. T.; Clancy, P.; Bao, Z.; Amassian, A. Nat. Commun. 2014, 5, 3573.

(32) Wo, S.; Headrick, R. L.; Anthony, J. E. *J. Appl. Phys.* **2012**, *111*, 073716.

(33) Sutton, A. P.; Balluffi, R. W. *Interfaces in Crystalline Materials*; Oxford University Press, 1995.

(34) Taylor, G. *Proc. R. Soc. London, Ser. A* **1934**, *145*, 388.

(35) Hiszpanski, A. M.; Lee, S. S.; Wang, H.; Woll, A. R.; Nuckolls, C.; Loo, Y.-L. *ACS Nano* **2013**, *7*, 294.

(36) Kim, K.; Rho, Y.; Kim, Y.; Kim, S. H.; Hahm, S. G.; Park, C. E. *Adv. Mater.* **2016**, *28*, 3209.

(37) Li, H.; Tee, B. C.; Giri, G.; Chung, J. W.; Lee, S. Y.; Bao, Z. *Adv. Mater.* **2012**, *24*, 2588.